

APPLICATIONS OF A NEW CODE TO COMPUTE TRANSFER MAPS AND DESCRIBE SYNCHROTRON RADIATION *

D. Newton[†] and A. Wolski, University of Liverpool, and the Cockcroft Institute, UK.

Abstract

An analytic tracking code has been developed to describe an arbitrary magnetic field in terms of its generalised gradients [1] and multipole expansion, which is used with a second order symplectic integrator [2] to calculate dynamical maps for particle tracking. The modular nature of the code permits a high degree of flexibility and allows customised modules to be integrated within the code framework. Several different applications are presented, and the speed, accuracy and flexibility of the algorithms are demonstrated. A module to simulate synchrotron radiation emission is described, and its application to a helical undulator is demonstrated.

INTRODUCTION

Analytical descriptions of magnetic fields offer many advantages over numerical maps. Explicitly describing field components allows a deeper understanding of charged particle dynamics, and the ability to generate transfer maps gives huge speed advantages in particle tracking and lattice analysis. However, accurately describing higher-order (non-linear) components of “real” magnets has historically been a challenging problem. Often an assumption is made that the magnet is ideal or pseudo-ideal. While this assumption is often valid, more realistic analytic descriptions of magnetic fields can be of particularly importance for novel magnet designs, where non-linear terms give a significant contribution to the total field. Analytic descriptions also provide significant advantages for long undulator systems with strong fringe field contributions, where numerical tracking schemes can be laborious. A technique to describe analytically an arbitrary magnetic field is given by Venturini and Dragt [1], and has been implemented in a C++ code [3] along with a second order symplectic integrator [2]. This code allows fast, accurate numerical or analytic particle tracking through arbitrary magnetic fields. In this paper, some applications of the code are discussed. A module to describe synchrotron radiation has been added, and some results using both ideal and “real” magnet systems are presented.

SYNCHROTRON RADIATION EMISSION

To compute the emission of synchrotron radiation, a particle is tracked numerically in the manner described in reference [3], but at each integration step, the effective radius

of curvature of the particle is estimated, and the resulting electric field is calculated at a pre-defined observation point. The electric field induced by an accelerated charge is given by:

$$\vec{E}(t) = \frac{e}{4\pi\epsilon_0 c} \frac{1}{(1 - \vec{n} \cdot \vec{\beta})^3} \times \left(\frac{(1 - |\vec{\beta}|^2)(\vec{n} - \vec{\beta})}{|\vec{R}|^2} + \frac{\vec{n} \times [(\vec{n} - \vec{\beta}) \times \dot{\vec{\beta}}]}{c|\vec{R}|} \right)_{RET}, \quad (1)$$

where \vec{R} is the vector from the charged particle to the observation point, with unit vector \vec{n} [4], and the other symbols have their usual meaning. A Fourier transform of the resultant field gives the frequency spectrum:

$$\begin{aligned} \frac{d^2 U}{d\Omega dt} &= \epsilon_0 c E^2 r^2 = \vec{G}(t)^2 \\ \vec{G}(\omega) &= \frac{1}{\sqrt{2\pi}} \int_{-\infty}^{\infty} \vec{G}(t) \exp(i\omega t) dt \\ \frac{d^2 I}{d\Omega d\omega} &= |\vec{G}(\omega)|^2 + |\vec{G}(-\omega)|^2 \end{aligned}$$

The electric field data, including the polarisation state, are calculated at each step and saved in a ROOT TTree object [5]. This format is designed for storing large quantities of data and is optimised to reduce disk space and enhance access speed. It also offers a flexible method of inspecting and plotting the raw data, and periodically writes to a file during long calculations, safeguarding against system failures and reducing the necessary memory cache.

Comparison with an analytic calculation

The frequency distribution of radiation emitted by a charged particle in circular motion can be calculated analytically [4], allowing a comparison with the numerical calculation. Using the code described in reference [3], an ideal normal dipole field with strength 1 T was characterised and an electron of energy 100 MeV was tracked through 10,000 integration steps using a second order symplectic integrator. Fig. 1 shows the evolution of the dynamical variables x (the horizontal coordinate) and s (the longitudinal coordinate relative to a reference particle). In such a field, the particle describes an arc of radius ~ 0.33 m in the $x - z$ plane. At an observation point ($x = 0, y = 0, z = 0.1$) in the coordinate frame of Fig. 1, the frequency distribution was calculated analytically and compared to the numerical result.

* Work supported by the Science and Technology Facilities Council, UK.

[†] david.newton@stfc.ac.uk

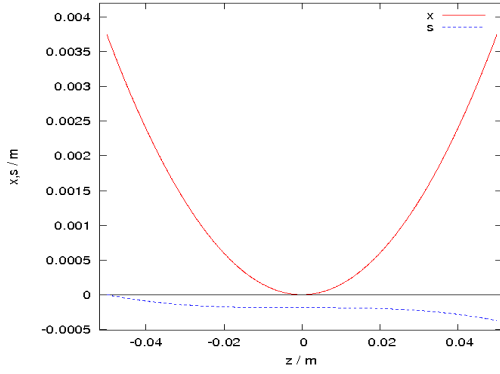


Figure 1: The phase space coordinates x and s for a 100 MeV electron in a dipole field of 1 T.

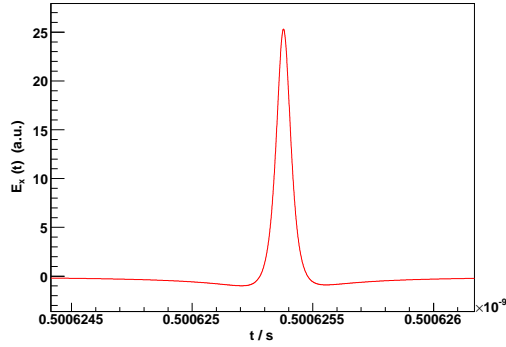


Figure 2: The calculated electric pulse due to an electron in a circular orbit. The observation point is in the same plane as the electron's path, so only the x -component of the electric field is present.

Fig. 2 shows the electric field as a function of time, calculated using Eq. (1). The frequency spectrum is obtained by a Fourier transform: the result is shown in Fig. 3. The analytical result is also plotted: the analytical spectrum has a peak value of $3.300 \times 10^{-33} \text{ J Sr}^{-1} \text{ s}^{-1}$ at $1.339 \times 10^{15} \text{ Hz}$, which is also where the maximum discrepancy between the two curves occurs. The calculated value differs from the analytical value by $\sim 1.6 \times 10^{-36}$, giving an agreement between the two of better than 0.05%.

APPLICATION TO THE ILC HELICAL UNDULATOR

The ILC positron source [6] is based on the generation of 10 MeV photons by passing a 150 GeV electron beam transported through a 150 m helical undulator. The helical undulator will have a periodicity of 1.15 cm, with each module containing 155 periods, giving a module length of 1.79 m.

A numerically calculated field map of a single period of the undulator system (Fig. 4) was used as an input map for the code. Following the procedure outlined in reference [3], the generalised gradients were calculated and used to

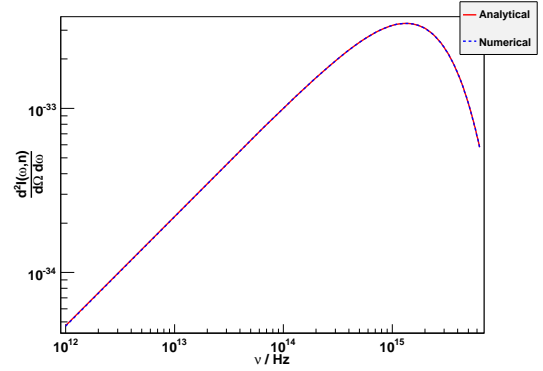


Figure 3: The differential power spectrum for an electron in a circular orbit, measured in J Sr^{-1} , radiated into unit frequency interval. The analytical and numerical curves agree within 0.05%.

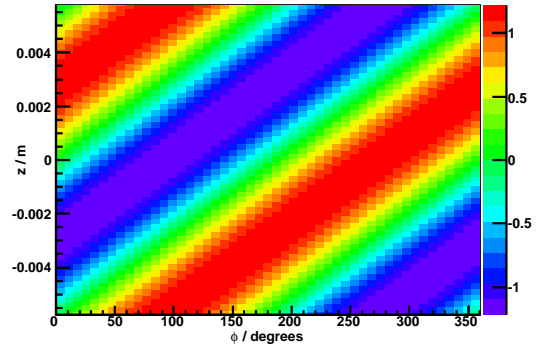


Figure 4: The radial component of the magnetic field in a helical undulator with periodicity 0.115 m, projected onto the surface of a cylinder of radius 0.0019 m.

generate an analytical description of the vector potential. Finally the phase space vector $(x, p_x, y, p_y, s, \delta)$ was integrated over the length of the undulator system. The normal and skew on-axis generalised gradients $C_{1,s}^{[0]}$ and $C_{1,c}^{[0]}$, corresponding to the on-axis field components B_y (normal) and B_x (skew), are shown in Fig. 5. Fig. 6 shows the result of tracking numerically the phase space vector through a single period of the undulator. The dynamical variables were integrated over one period using 10,000 integration steps, although the electric field was only calculated every 10th step. The speed of this operation could be improved by analytically integrating a transfer matrix over every 10 steps and writing the result to a file. Once this is done, the numerical integration can be achieved using only 1000 steps, with no loss of accuracy, for any initial phase space coordinates.

The frequency distribution of synchrotron radiation emitted by a 150 GeV electron moving through a 1.79 m helical undulator of 155 periods, observed at an observation point 10 m (on-axis) from the end of the undulator was calculated using 1.55×10^6 integration steps, with the electric field calculated every 10th step. The start-to-end calcu-

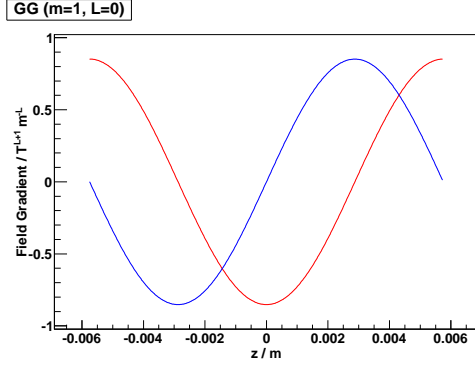


Figure 5: The normal (red) and skew (blue) dipole components of the generalised gradients $C_{1,s}^{[0]}$ and $C_{1,c}^{[0]}$ for the helical undulator. These components are identified with the on-axis fields B_y and B_x .

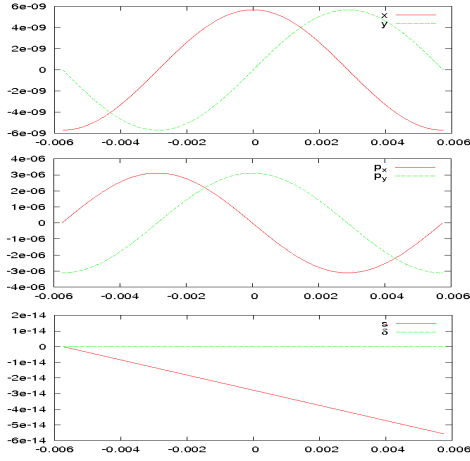


Figure 6: The evolution of the phase space vector $(x, p_x, y, p_y, s, \delta)$ as a 150 GeV electron traverses one period of the helical undulator with field shown in Fig. 4.

lation took just under 15 minutes on a 2.66 GHz processor. A section of the x -component of the field is shown in Fig. 7. The total pulse had a duration of 8×10^{-20} s. Following a Fourier transform the energy spectrum is shown in Fig. 8, with a strong harmonic at 10.1 MeV.

CONCLUSION

The C++ code described here and in reference [3] is designed to give a fast, accurate method of characterising magnetic fields, performing numerical particle tracking, and calculating analytic transfer maps. The code is still in the development phase – for example, the synchrotron radiation module in particular is not yet optimised. The modular design allows additional functionality to be implemented with minimum reprogramming. The ability to calculate analytic transfer maps means that the synchrotron radiation module can be optimised to reduce the number of calculations, with no loss of accuracy in the tracking code.

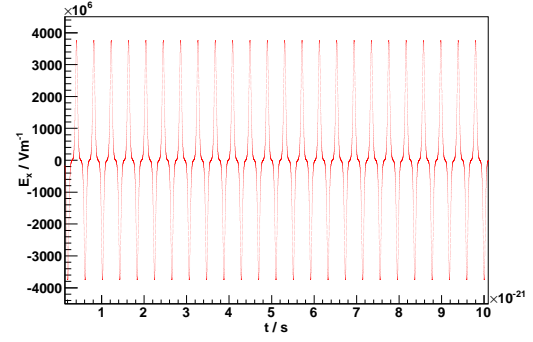


Figure 7: A portion of the x -component of the electric field, observed 10 m from the end of a 1.79 m helical undulator (155 periods).

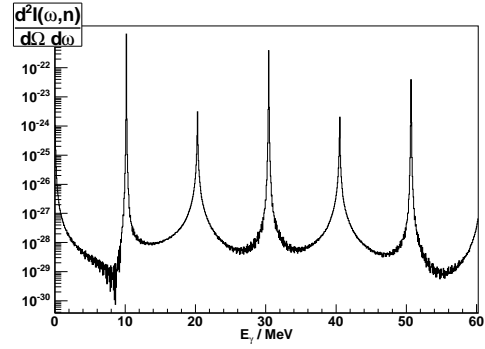


Figure 8: The photon energy distribution of radiation emitted by a 150 GeV electron passing through one section (1.79 m, 155 periods) of a helical undulator. The first harmonic occurs at a photon energy of 10.1 MeV.

The calculation can also be started at any point within the magnet system, making the code ideally suited to parallel or pseudo-parallel (e.g. Condor) applications.

REFERENCES

- [1] M. Venturini and A.J. Dragt, “Accurate computation of transfer maps from magnetic field data”, Nuclear Instruments and Methods in Physics Research A, 429 (1999), 387-392.
- [2] Y. Wu, E. Forest, and D.S. Robin, “Explicit higher order symplectic integrator for s -dependent magnetic field”, Phys. Rev. E 68, 046502 (2003).
- [3] D. Newton and A. Wolski, “Fast, accurate calculation of dynamical maps from magnetic field data using generalised gradients”, these proceedings.
- [4] J.D. Jackson, “Classical Electrodynamics”, third edition, John Wiley & Sons, 1999, Chapter 14.
- [5] Rene Brun and Fons Rademakers, “ROOT - An Object Oriented Data Analysis Framework”, Proceedings AIHENP’96 Workshop, Lausanne, Sep. 1996, Nuclear Instruments and Methods in Physics Research A 389 (1997) 81-86. See also <http://root.cern.ch/>
- [6] ILC Reference Design Report (2007). <http://www.linearcollider.org/cms/?pid=1000437>